Fatima M. Ahmed [1]
Khalil I. Mohammed [2]
Rafea A. Munef [1]

[1] Department of Physics, College of Science, University of Kirkuk, Kirkuk, IRAQ
[2] Department of Physics, College of Education for Pure Science, University of Kirkuk, Kirkuk, IRAQ

Investigation of Physical Properties of Cobalt Nanoparticles Synthesized via Pulsed Laser Ablation in Liquid

Cobalt nanoparticles with 99.99% purity were synthesized from cobalt flakes using pulsed laser ablation in liquid with a Nd:YAG laser. Two laser wavelengths (532 and 1064 nm) and various laser fluences (30, 40, 50, and 60 J/cm²) were employed, with 300 pulses at a 6 Hz repetition rate. The UV-visible spectroscopy revealed optical absorption peaks in the range of 270-297 nm. The x-ray diffraction analysis confirmed that the cobalt nanoparticles exhibit a cubic crystalline structure. Atomic force microscopy showed that increasing laser fluence reduced the particle size. Field-emission scanning electron microscopy images revealed nanoparticles with an average diameter of approximately 18.17 nm. These results indicate that laser fluence plays a crucial role in controlling the size and physical properties of the cobalt nanoparticles produced.

***Keywords*:** Cobalt; Nanoparticles; Surface plasmon resonance; Laser-induced oxidation
Received: 16 August 2024; **Revised:** 15 October 2024; **Accepted:** 22 October 2024

1. Introduction

Nanoparticles are tiny particles with diameters ranging from 1 to 100 nm, exhibiting properties distinct from their bulk counterparts [1]. At the nanoscale, materials acquire unique advantages, primarily due to a significant increase in surface area and surface activity [2]. As the size of a material decreases, it becomes more influenced by the behavior of its fundamental constituents, namely atoms and molecules. This results in properties that differ markedly from those of bulk materials, including changes in melting point, dielectric constant, and alterations in activity, solubility, and mass and heat transfer dynamics. These differences stem from the modified bonding interactions within nanoparticles, particularly at their highly active surfaces [3]. The physics and chemistry of metal nanoparticles are largely governed by their size, shape, and composition, making precise control over these parameters critical for optimizing performance [4,5].

Nanoparticles are fundamental to nanotechnology, with applications in biosensors, electronic devices, and beyond [6,7]. Their electrical, optical, magnetic, and chemical properties differ significantly from bulk materials due to their large surface area-to-volume ratio, quantum confinement effects, and surface plasmon resonance (SPR) [8-11]. Metal nanoparticles, particularly those between 10 to 100 nm, exhibit distinctive SPR and optical characteristics [12]. The vivid colors of noble metal nanoparticles arise from the resonant excitation of collective electron oscillations, or particle plasmons, and their surface plasmon resonance (SPR) absorption is influenced by size, shape, and composition [13].

Laser ablation offers a clean, chemical-free method for producing high-purity nanoparticles through a simple, cost-effective process [14,15]. This top-down physical approach involves breaking down bulk metal precursors into metal atoms [16,17]. Laser ablation in liquids is an innovative and versatile method for synthesizing diverse nanomaterials. Its core advantage lies in the nonequilibrium growth process triggered by the transient plasma generated when the laser hits the target material immersed in a solution [18]. This plasma exhibits extremely high temperatures, pressures, and concentrations of excited particles [19]. Whether lasers merely cut or engrave or push the boundaries to burning, melting, boiling, and even turning to plasma, the backing material laser interaction outcomes stem from power and timing exposure [20,21].

This research project investigates the sizing and characterization of cobalt nanoparticles synthesized by pulsed laser ablation in liquid. The significance of this study lies in the fact that if one could control the size and purity during the synthesis process, such nanoparticles would be ideally suited for chemical, magnetic, and biomedical applications; thus, it is necessary to understand the factors of laser and laser parameters for creation that impact such sizes and characteristics.

2. Materials and Methods

Cobalt nanoparticles (Co NPs) were synthesized through pulsed laser ablation in liquid (PLAL). Before the ablation process, a cobalt plate with 99.99% purity was ultrasonically cleaned in a methanol bath for 10 minutes to remove surface impurities, followed by an acetone rinse to eliminate any remaining organic contaminants. The plate was then thoroughly rinsed with deionized water (DI-water) [3].

For the ablation process, cobalt plates, each with dimensions of 1×1×1 cm, were immersed in 3 mL of DI-water in a beaker. The target was positioned 5 cm away from the laser source. A quartz convex lens was used to focus the laser beam, which had a diameter of 10 mm, onto the cobalt object surface. The laser employed was a Q-switched Nd:YAG emitting at 1064 and 532 nm, operating at a pulse duration of 9 ns. A total of 300 pulses were applied at a repetition rate of 6 Hz, with varying laser fluences of 30, 40, 50, and 60 J/cm², as illustrated in Fig. (1) [3].

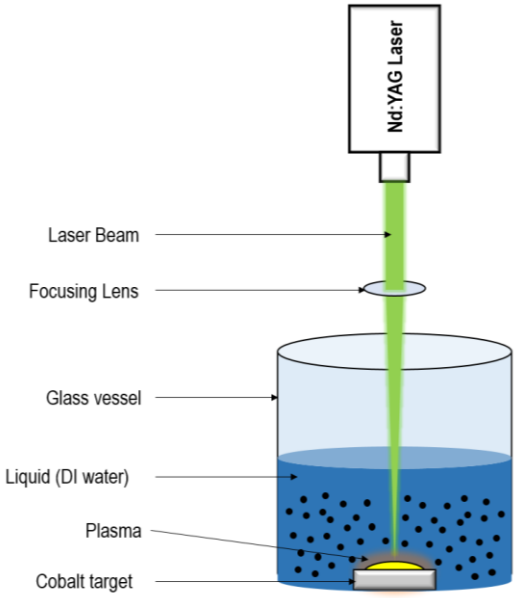

Fig. (1) Schematic illustration of Co NPs formation by Nd:YAG PLAL method

3. Results and Discussions

The identification of various substances, including transition metal ions, organic compounds, and biomolecules, commonly relies on optical techniques such as UV-visible spectroscopy. In this study, the synthesis of cobalt nanoparticles is indicated by a noticeable color change in the colloidal solution, transitioning from colorless to light yellowish-brown (Fig. 2). This change is directly linked to the cobalt ablation process and reflects the formation of cobalt nanoparticles, as the color of the colloid is influenced by the nanoparticle size and concentration [22-25].

The initial characterization of cobalt nanoparticles and their oxides was conducted using UV-visible spectroscopy, with detection facilitated by an Nd:YAG laser. The experiment utilized laser wavelengths of 532 and 1064 nm, with a total of 300 pulses. It was observed that as the laser fluence increased (30, 40, 50, and 60 J/cm²), the maximum absorption decreased. The surface plasmon resonance (SPR) spectrum of the cobalt nanoparticles solution displayed a semi-symmetric absorption band between 270 and 297 nm, indicative of spherical nanoparticles in the growth solution (Fig. 3). The maximum absorptions at 1064 nm exceeded those using 532 nm wavelength. Specifically, using 532 nm wavelength and 40 J/cm², the highest absorption was 0.0625, while at 1064 nm and the same fluence, the maximum absorption was 0.0633, both decreasing with higher laser fluences. This suggests that at 1064 nm, the cobalt nanoparticles were smaller compared to those produced using 532 nm wavelength, where the strongest surface plasmon resonance (SPR) absorption was detected.

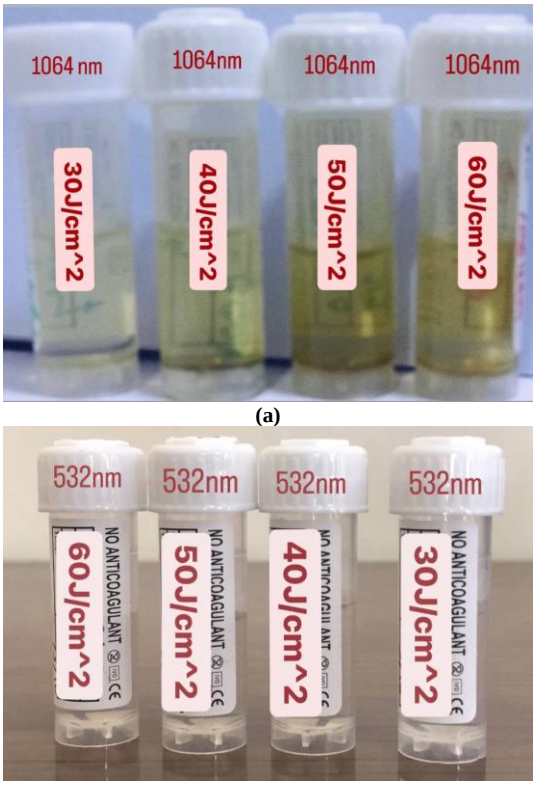

Fig. (2) Photograph of colloidal solutions colors of prepared Co NPs with different laser fluences (30-40-50-60) J/cm² using (a) wavelength 532 nm (b) wavelength 1064 nm

Additionally, cobalt (II, III) oxide, or tricobalt tetroxide (Co_3O_4), is identified with a cubic crystalline structure (Fig. 4), as referenced by JCPDS card no. 01-080-1536, and shows 2θ peaks at 19.257°, 36.35°, 44.90°, 58.83°, and 72.49°. The observed crystal planes for these angles are (111), (222), (311), (400), (511), and (620) [26-28].

Moreover, cobalt nanoparticles exhibit both hexagonal and cubic phases, as indicated by 2θ angles at 27.2°, 41.016°, 44.557°, 46.7°, 47.6°, 63.005°, and 75.8°. These peaks correspond to the (110), (100), (002), (011), (101), (102), and (110) crystal planes, consistent with JCPDS card no. 01-089-4308, JCPDS card no. 00-001-1278, and JCPDS card no. 69-901-1618 [29]. These results align with the previously published findings [30-32]. The average crystallite

sizes (D_{ave}), calculated using the Debye-Scherrer (Eq. 1), are detailed in table (1) [33]

$$D_{ave} = \frac{k\lambda}{\beta \cos\theta} \quad (1)$$

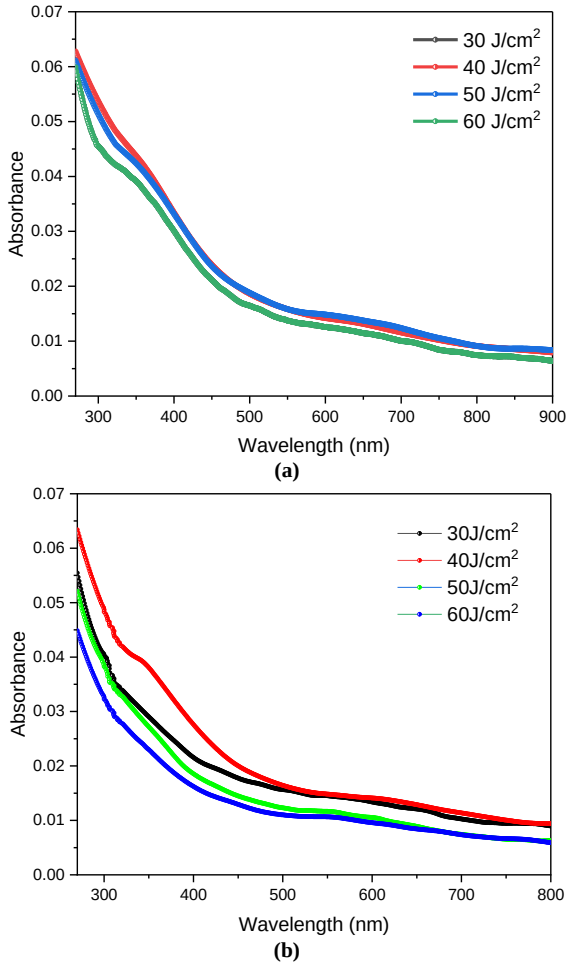

Fig. (3) Optical absorption of Co NPs with different laser fluences (30-40-50-60) J/cm^2 using (a) wavelength 532 nm (b) wavelength 1064 nm

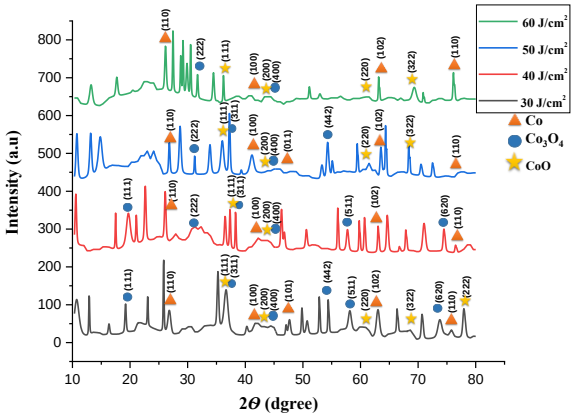

Fig. (4) XRD patterns of Co NPs prepared with different laser fluences using 1064nm laser wavelength

The laser-induced oxidation effect is an inevitable result of the interaction between the laser beam and metals when exposed to air. This influence is primarily due to the elevated temperatures generated during laser exposure, which cause rapid thermal diffusion into the surrounding environment. The heat dissipates quickly, allowing thermal energy to extend beyond the immediate laser-exposed region, oxidizing the metal surface outside the ablation zone. Studies show that this process alters the chemical composition of the metal surface due to net atomic mobility [18]. The ablated material undergoes melting and evaporation within nanoseconds, expanding into the surrounding plasma as it interacts with the ambient gas. This high-temperature treatment facilitates the oxidation of the resulting nanoparticles. These observations are consistent with the findings of Fernández-Arias et al. [34], further supporting the role of thermal diffusion in promoting oxidation during laser ablation.

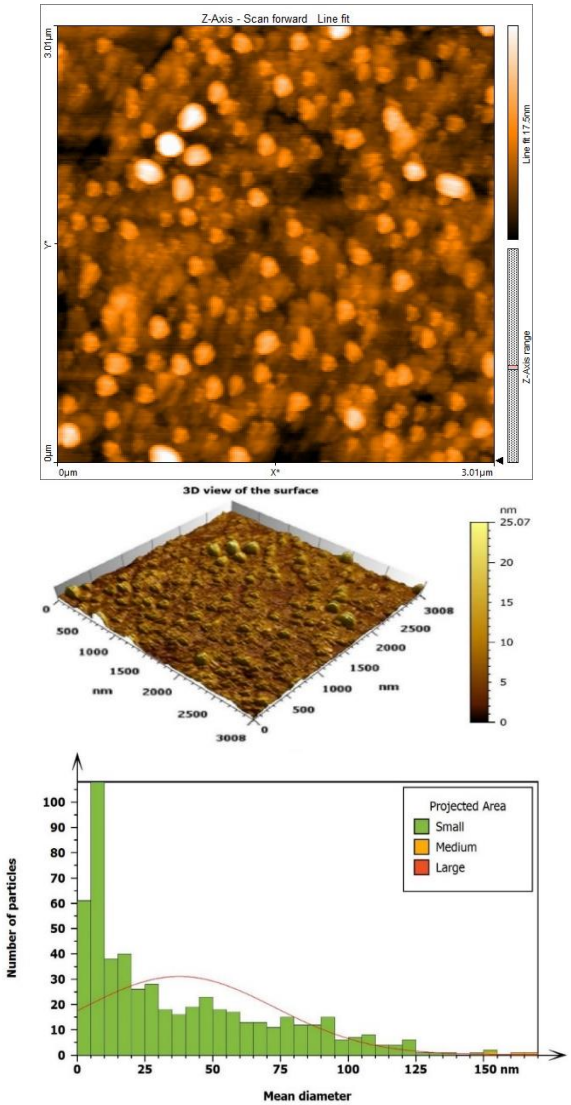

Fig. (5) AFM images of Co NPs prepared with 40 J/cm^2 laser fluence using laser wavelength of 1064nm

The topography of the cobalt nanoparticles structure, prepared using a 1064 nm wavelength, a laser

fluence of 40 J/cm², and 300 laser pulses, was analyzed using atomic force microscopy (AFM). The root mean square (RMS) roughness and surface roughness were determined from the 2D and 3D AFM images, as shown in Fig. (5). The results revealed that the average particle diameter was 170.0 nm, with an average roughness of 42.44 nm, defined as the difference between the highest and lowest surface peaks. The RMS value, which measures the average height of these peaks, was found to be 54.13 nm. This value reflects the overall variation in height across the surface of the nanoparticles.

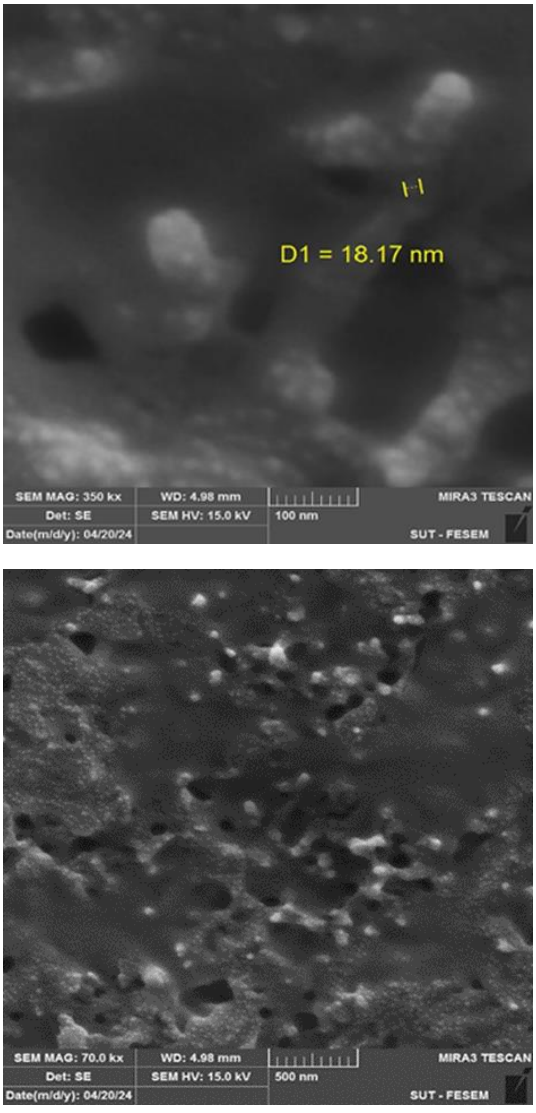

Fig. (6) FE-SEM images of Co nanoparticles prepared with 40 J/cm² laser fluence using laser wavelength of 1064nm

The increase in surface roughness is attributed to the tendency of particles to agglomerate due to collisional motion, as matter naturally seeks stability [35,36]. This agglomeration leads to larger nanoparticles, consequently increasing both the surface roughness and surface area. In the 2D AFM image, a color gradient is used to represent nanoparticle size, with darker regions indicating smaller particles and lighter regions representing larger particles [3,37]. These observations suggest that the laser ablation parameters significantly influence the surface morphology and nanoparticle size distribution.

Field-emission scanning electron microscopy (FE-SEM) was performed on cobalt nanoparticles synthesized using a laser wavelength of 1064 nm and a fluence of 40 J/cm² to assess their dimensions and morphology. The analysis confirms the successful production of nanoscale particles. Figure (6) depict the morphological features, shapes, and size distributions of the cobalt nanoparticles produced via pulsed laser ablation in liquid (PLAL).

The images are shown at two different scales (100 and 500 nm), clearly illustrating the spherical shape of the nanoparticles. This spherical morphology is consistent with the single surface plasmon resonance (SPR) peaks observed in the absorption spectra, aligning with the results reported by Jasim et al. [18]. The average diameter of the nanoparticles was determined to be 18.17 nm.

4. Conclusions

Cobalt nanoparticles were successfully synthesized using pulsed laser ablation in liquid (PLAL). Cobalt was ablated using an Nd:YAG laser using 532 and 1064 nm wavelengths at varying fluences and 300 pulses. The nanoparticles were formed as evidenced by the color change of the solution, and surface plasmon resonance measurements gave peaks at 532 nm (0.0625 absorbance) and 1064 nm (0.0633 absorbance) indicating perfect formation. Furthermore, the FE-SEM images of cobalt nanoparticles suggest that the nanoparticles are primarily spherical in nature with an average size of 18.17 nm. AFM results showed slightly larger particle sizes compared to FE-SEM, which can be attributed to nanoparticle agglomeration. This discrepancy underscores the importance of considering agglomeration effects when interpreting nanoparticle size measurements.

References

[1] R.A. Munef, "pH Effect on Structural and Optical Properties of Nanostructured Zinc Oxide Thin Films", *Proc. AIP Conf.*, 1653 (2015) 020075.

[2] A.M.K. Albayati, R.A. Munef and R.M.S. Alhaddad, "Shape and Size Effect of Surface Plasmons on Gold Nanoparticles", *Syst. Rev. Pharm.*, 11(11) (2020) 507-514.

[3] N.M.A. Fadhil and F.M. Jasim, "Study of Optical and Structural Properties of Prepared Gold Nanoparticles by Pulsed Laser Ablation Method," *J. Educ. Sci.*, 30(4) (2021) 69-82.

[4] S.L. Logunov et al., "Electron Dynamics of Passivated Gold Nanocrystals Probed by Subpicosecond Transient Absorption Spectroscopy", *J. Phys. Chem. B*, 101(19) (1997)

3713-3719.
[5] C. Burda et al., "Chemistry and Properties of Nanocrystals of Different Shapes", *Chem. Rev.*, 105(4) (2005) 1025-1102.
[6] D.K. Naser, A.K. Abbas and K.A. Aadim, "Zeta Potential of Ag, Cu, ZnO, CdO and Sn Nanoparticles Prepared by Pulsed Laser Ablation in Liquid Environment", *Iraqi J. Sci.*, 61(10) (2020) 2570-2581.
[7] M.H. Yaseen, R.J. Hameed and A.M. Jasim, "Energy Band Outline of Thin Film CoO:Au/Si Solar Cells", *Iraqi J. Mater.*, 1(2) (2022) 89-94.
[8] V. Piriyawong et al., "Effect of Laser Pulse Energy on the Formation of Alumina Nanoparticles Synthesized by Laser Ablation in Water", *Procedia Eng.*, 32 (2012) 1107-1112.
[9] R.A. Munef, B.A. Omar and S.J. Fathi, "Preparation and Synthesis of the Nanoferrite $Ni_{0.3}Co_{0.2}Zn_{0.5}Al_xFe_{2-x}O_4$ Utilizing Sol-Gel Auto-Combustion Approach", *J. Ovonic Res.*, 18(2) (2022) 213-218.
[10] D. Mirela, "Metallic Nanoparticles", Univ. Nov. Goric. (2009), pp. 3765-3775.
[11] N.A.H. Hashim and F.J. Kadhim, "Structural and Optical Characteristics of Co_3O_4 Nanostructures Prepared by DC Reactive Magnetron Sputtering", *Iraqi J. Appl. Phys.*, 18(4) (2022) 31-36.
[12] H. Kumar et al., "Metallic Nanoparticle: A Review", *Biomed. J. Sci. Tech. Res.*, 4(2) (2018) 3765-3775.
[13] M.I. Mendivil et al., "Transmission Electron Microscopic Studies on Noble Metal Nanoparticles Synthesized by Pulsed Laser Ablation in Liquid", *Microsc. Adv. Sci. Res. Educ.*, 1 (2014) 911-920.
[14] M.Z. Alhamid, B.S. Hadi and A. Khumaeni, "Synthesis of Silver Nanoparticles Using Laser Ablation Method Utilizing Nd:YAG Laser", *Proc. AIP Conf.*, 2202 (2019) 020013.
[15] W.S. Suleiman and K.I. Muhammad, "Study of the Optical Properties of Silver Nanoparticles Prepared by the Pulsed Laser Ablation Technique in Water", *Int. J. Sci. Res. Sci. Technol.*, 10(4) (2023) 531-537.
[16] H.H. Bahjat et al., "Magnetic Field-Assisted Laser Ablation of Titanium Dioxide Nanoparticles in Water for Anti-Bacterial Applications", *J. Inorg. Organomet. Polym. Mater.*, 31(9) (2021) 3649-3656.
[17] W. Norsyuhada et al., "Synthesis and Characterization of Gold-Silver Nanoparticles in Deionized Water by Pulsed Laser Ablation (PLAL) Technique at Different Laser Parameters", *Int. J. Nanosci.*, 18(01) (2019) 1850015.
[18] A.S. Jasim, K.A. Aadim and S.N. Rashid, "Optical and Structural Properties of Cobalt Nanoparticles Synthesized by Laser Ablation", *Iraqi J. Sci.*, 63(10) (2022) 4292-4304.
[19] H. Zeng, S. Yang and W. Cai, "Reshaping Formation and Luminescence Evolution of ZnO Quantum Dots by Laser-Induced Fragmentation in Liquid", *J. Phys. Chem. C*, 115(12) (2011) 5038-5043.
[20] A.H. Hamad, "Picosecond Laser Generation and Modification of Ag-TiO_2 Nanoparticles for Antibacterial Application", The University of Manchester (2017).
[21] K.A. Aadim, "Characterization of Laser Induced Cadmium Plasma in Air", *Iraqi J. Sci.*, 56(3B) (2015) 2292-2296.
[22] H.H. Bahjat, R.A. Ismail and G.M. Sulaiman, "Photodetection Properties of Populated Fe_3O_4@ TiO_2 Core-Shell/Si Heterojunction Prepared by Laser Ablation in Water", *Appl. Phys. A*, 128(1) (2022) 8.
[23] K. Maaz, **"Cobalt"**, InTech Open (Croatia, 2017), Ch. 4, p. 56.
[24] A.E. Kaloyeros et al., "Review–cobalt thin films: trends in processing technologies and emerging applications", *ECS J. Solid State Sci. Technol.*, 8 (2019) 119.
[25] R. Lakra et al., "Synthesis and characterization of cobalt oxide (Co_3O_4) nanoparticles", *Mater. Today: Proc.*, 2 September 2020.
[26] H.E. Swanson, M.C. Morris and E.H. Evans, "Standard X-ray diffraction powder patterns", U.S Department of Commerce, National Bureau of Standards, vol. 9 (1960) pp. 28-29.
[27] O.A. Hammadi and N.E. Naji, "Fabrication and Characterization of Polycrystalline Nickel Cobaltite Nanostructures Prepared by Plasma Sputtering as Gas Sensor", *Phot. Sen.*, 8(1) (2018) 43-47.
[28] N.A.H. Hashim, F.J. Kadhim and Z.S. Abdulsattar, "Characterization of Electrochromism and Photoelectrochromism of N-Doped TiO_2 and Co_3O_4 Thin Films Prepared by DC Reactive Magnetron Sputtering: Comparative Study", *Iraqi J. Appl. Phys.*, 19(1) (2023) 5-12.
[29] H.E. Swnason et al., **"Standard X-Ray Diffraction Powder Patterns"**, International Center for Diffraction Data (ICDD) (Washington DC, 1971), NBS monograph 25, Sec. 9, p. 29
[30] V. Patil et al., "Synthesis and Characterization of Co_3O_4 Thin Film", *Sci. Res.*, 2(1) (2012) 1-7.
[31] H. Heli and H. Yadegari, "Nanoflakes of the cobaltous oxide, CoO: Synthesis and characterization", *Electrochimica Acta*, 55 (2010) 2139-2148.
[32] H.E. Swanson, M.C. Morris and E.H. Evans, "Standard X-ray diffraction powder patterns", U.S Department of Commerce, National Bureau of Standards, vol. 25, sec. 4, (1966) pp. 10-14.
[33] B.D. Cullity and S.R. Stock, "Elements of X-Ray Diffraction", 3rd ed., Pearson (London, 2014), Ch.

20, p. 615.
[34] M. Fernández-Arias et al., "Fabrication and Deposition of Copper and Copper Oxide Nanoparticles by Laser Ablation in Open Air", *Nanomaterials*, 10(2) (2020) 300.
[35] W.A. Al-Daim, G.A. Al-Dahash and Z. Laith, "Synthesis Conditions of Au Core@ Ag Shell System by Laser Ablation in Distilled Water Using Different Wavelengths (1064, 532, 355) nm", *Proc. J. Phys.: Conf. Ser.*, (2019) 12010.
[36] S.C. Endres, L.C. Ciacch and L. Madler, "A review of contact force models between nanoparticles in agglomerates, aggregates and films", *J. Aerosol Sci.*, 153 (2021) 105719.
[37] X. Zhu et al., "Co_3O_4 nanoparticles with different morphologies for catalytic removal of ethyl acetate", *Catal. Comm.*, 156 (2021) 106320.

Table (1) Results of XRD analysis of cobalt nanoparticles synthesized in this work

Wavelength (nm)	Sample	Laser Fluence (J/cm^2)	2θ (deg)	hkl	FWHM [2θ]	Crystal Size (nm)	Average Crystalline Size (nm)
1064	Co	30-40-50-60	27. 200	110	0.476	17.5	16.11429
			41.016	100	1.1808	7.2	
			44.557	002	2.361	3.6	
			46.700	011	0.3936	22.3	
			47. 600	101	0.1968	46	
			63.005	102	0.9840	9.5	
			75.800	110	1.440	6.7	
1064	CoO	30-40-50-60	37.425	111	0.2952	29.2	28.02
			41.125	200	0.7828	10.9	
			60.773	220	1.5744	5.9	
			74.100	311	0.1476	67.4	
			77.885	222	0.3600	27	
1064	Co_3O_4	30-40-50-60	19.257	111	1.5744	5.1	24.22
			36.350	311	0.7872	10.7	
			44.900	400	1.5755	5.5	
			58.830	511	0.1475	66.1	
			72.490	620	0.3000	33.7	

